Bioresource Technology 439 (2026) 133319

Contents lists available at ScienceDirect

Bioresource Technology

journal homepage: www.elsevier.com/locate/biortech

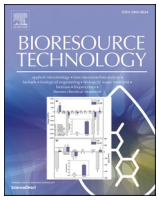

# Production of Ultraviolet A protectant C50 carotenoid decaprenoxanthin by metabolically engineered *Corynebacterium glutamicum*☆

Fynn Stegelmann [a], Jan Seeger [a], Petra Peters-Wendisch [a], Nadja A. Henke [b], Volker F. Wendisch [a,*]

[a] Genetics of Prokaryotes, Faculty of Biology and Center for Biotechnology (CeBiTec), Bielefeld University, Universitaetsstr. 25, D-33615 Bielefeld, Germany
[b] Institute for Process Engineering in Life Sciences, Karlsruhe Institute of Technology (KIT), Kaiserstraße 12, 76131 Karlsruhe, Germany

## HIGHLIGHTS

- Gram-*per*-liter production of decaprenoxanthin enabled.
- *crtX* overexpression increased glucosylation status of decaprenoxanthin.
- Sustainable decaprenoxanthin production from food waste hydrolysate established.
- Efficient extraction of decaprenoxanthin from biomass with green solvent ethanol.
- First antioxidative activity determination of decaprenoxanthin and glucosides.

## GRAPHICAL ABSTRACT

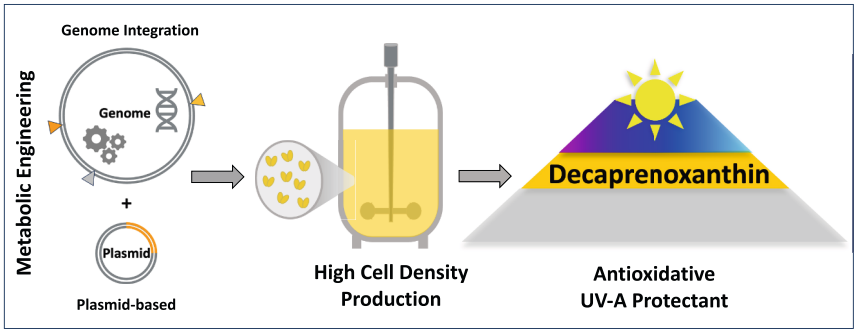


## ARTICLE INFO

*Keywords:*
Antioxidative activity
Alternative carbon sources
Fed-batch fermentation

## ABSTRACT

Carotenoids play roles as active compounds in cosmetics, food, and feed applications, for which C40 carotenoids are most common. In recent years, *Corynebacterium glutamicum*, a Gram-positive bacterium renowned for large-scale amino acid processes, has been engineered to produce various C40 carotenoids such as the high value astaxanthin. In contrast, the native glucosylated C50 carotenoid decaprenoxanthin of *C. glutamicum* remained rather unexplored. Here, by using genome editing and plasmid-based overexpression of carotenogenic genes, 230 mg $L^{-1}$ decaprenoxanthin was produced in shake flasks. Transfer to a 2 L fed-batch fermentation yielded 1450 mg $L^{-1}$, the highest C50 carotenoid titer reported to date. Production on alternative carbon sources, solubility, glucosylation impact and antioxidative activity were investigated. The antioxidative activity of glucosylated decaprenoxanthin was higher than that of unglucosylated decaprenoxanthin. This work lays a foundation for the access to rare C50 carotenoids from *C. glutamicum* fermentation broth with a perspective towards higher production scales.

☆ This article is part of a special issue entitled: 'ICB-2025' published in Bioresource Technology.

* Corresponding author at: Genetics of Prokaryotes, Faculty of Biology and Center for Biotechnology (CeBiTec), Bielefeld University, Universitaetsstr. 25, D-33615 Bielefeld, Germany.
*E-mail address:* volker.wendisch@uni-bielefeld.de (V.F. Wendisch).

https://doi.org/10.1016/j.biortech.2025.133319
Received 17 July 2025; Received in revised form 9 September 2025; Accepted 9 September 2025
Available online 10 September 2025

## 1. Introduction

Carotenoids are renowned as colourful pigments, appearing in hues of red, orange, and yellow (Sandmann, 2021). In organisms, they serve physiological functions such as membrane stabilisation, photoprotection, light harvesting, and light sensing (Sandmann, 2019; Seel et al., 2020). Carotenoids are used as colorants in foods. Moreover, their photochemistry and radical-quenching abilities make them applicable for cosmetic products such as sunscreens and anti-ageing products, while medical applications for the treatment of cancer, diabetes, neurodegenerative, and inflammatory diseases are also discussed (Bin-Jumah et al., 2021; Sen and Chakraborty, 2011; Sigurdson et al., 2017). With rising consumer demands for natural products such as carotenoids, the global market size for synthetic and natural carotenoids of USD 2.5 billion is expected to grow to USD 3.4 billion by 2029 with an annual growth rate of 6.3 %. The market is dominated by carotenoids that are sourced from chemical synthesis (MarketsandMarketsTM, 2024; Research, 2024).

In nature, carotenoids containing alcohols as functional groups, making them part of the subgroup of xanthophylls, can be modified by glucosylation and/or esterification. Examples can be found in the glucosylated sioxanthin from *Salinispora tropica* or the esterified astaxanthin from *Haematococcus pluvalis* (Grung et al., 1992; Richter et al., 2015). Another example of a glucosylated carotenoid is decaprenoxanthin, the native carotenoid of the Gram-positive soil bacterium *Corynebacterium glutamicum*, which is mostly present as diglucoside (Andrewes and Liaaen-Jensen, 1984; Heider et al., 2014a). While *C. glutamicum* is renowned for its role in the million ton-scale industrial amino acid production, metabolic engineering of this bacterium broadened the portfolio of generally recognized as safe (GRAS) products and established access to alternative carbon sources (Zahoor et al., 2012). Notably, it has been engineered to produce non-native carotenoids such as the C40 carotenoids (Göttl et al., 2024; Henke et al., 2016; Li et al., 2021). C40 carotenoids are studied to a greater extent than C50 carotenoids. For example, *C. glutamicum* strains capable of producing lycopene, β-carotene, α-carotene, or astaxanthin have been developed (Göttl et al., 2024; Li et al., 2021). Besides their antioxidant activity, carotenoids are photoprotective (Sandmann, 2019). This photoprotective property led to the filing of a patent for the use of the C50 carotenoids sarcinaxanthin and decaprenoxanthin in sunscreens (Goksøyr, 2013). Beyond other natural ultraviolet (UV) protectants such as shinorine (Tsuge et al., 2018), decaprenoxanthin adds up to the portfolio produced by *C. glutamicum*.

By targeting the precursor supply in form of modifications to the methylerythritol 4-phosphate (MEP) pathway or by introducing the mevalonate (MVA) pathway, found in higher plants, fungi, and animals, the production of carotenoids and other terpenoids has been increased (Heider et al., 2014b; Henke et al., 2016; Luckie et al., 2024). Modifications to the downstream carotenoid synthesis have been made by introducing alterations to the *crt* operon of *C. glutamicum*, containing genes for the synthesis of the C40 precursor lycopene and the further synthesis of decaprenoxanthin (*crtYef* and crtEb), which were deleted in C40 producing strains to block conversion of lycopene (Heider et al., 2012). Addition of lycopene β-cyclase (*crtY*), β-carotene hydroxylase (*crtZ*), and β-carotene ketolase (*crtW*) genes allowed producing C40 astaxanthin and its precursors and intermediates (Heider et al., 2014a; Henke et al., 2016; Li et al., 2021). Bioreactor scale production of these strains have shown promising yields, with α-carotene and lutein production reaching the gram-*per*-liter scale (Eun et al., 2025; Li et al., 2024).

In this study, we adjusted the metabolic engineering strategies for production of heterologous carotenoids by *C. glutamicum* for overproduction of decaprenoxanthin from glucose and alternative carbon sources. Moreover, the glucosylation status was engineered and the impact of the glucosylation on solubility in water and the antioxidative activity was determined. Furthermore, production of decaprenoxanthin with gram-*per*-liter titers was shown to be transferable to the 2 L benchtop bioreactor scale and efficient extraction using the green solvent ethanol was established. To the best of our knowledge, the decaprenoxanthin titer of 1450 mg $L^{-1}$ is the highest product titer for a C50 carotenoid reported to date.

## 2. Materials and methods

### 2.1. Bacterial strains and growth conditions

*E. coli* DH5α and S17-1 were used for cloning and conjugation. Cultures were made with LB medium, under supplementation of respective antibiotics, at 37 °C and 180 rpm. *C. glutamicum* strains are listed in the Table S1. Precultures of *C. glutamicum* were prepared with LB, supplemented with 10 g $L^{-1}$ glucose and respective antibiotics at 30 °C and 120 rpm. Main cultures were prepared with CGXII minimal medium with 40 g $L^{-1}$ glucose, respective antibiotics, and 1 mM isopropyl β-D-1-thiogalactopyranoside (IPTG) when the inducible vectors pVWEx1, pECXT99A, or pEKEx3 were present. For the comparison of CGXII medium and trace salts (tr) (see Supplementary material) with the astaxanthin optimized CGAST1 medium and astaxanthin optimized trace salts (asta tr) (Meyer et al., 2025), combinations of the base media with the different trace salts were used for cultivation. Cultivations were done in 10 mL volumes in 100 mL baffled shake flasks. The used antibiotics tetracycline, kanamycin, and spectinomycin were added to concentrations of 5 μg $mL^{-1}$, 25 μg $mL^{-1}$, and 100 μg $mL^{-1}$ to the respective cultures. Nalidixic acid was used on selection plates for conjugation at a concentration of 50 μg $mL^{-1}$. All used antibiotics were supplied by VWR (Darmstadt, Germany). Other chemicals were supplied by Carl Roth (Karlsruhe, Germany).

### 2.2. Cloning and transformation of plasmids

Plasmids (Table S2) were constructed in *E. coli* DH5α. Target genes were amplified via polymerase chain reaction (PCR) (All-in HiFi, highQu, Kraichtal, Germany) using the oligonucleotides listed in Table S3, which were obtained from Metabion (Planegg/Steinkirchen, Germany). Sizes of amplicons were verified via gel electrophoresis in 1 % agarose TAE gels and purified using the Machery-Nagel (Düren, Germany) NucleoSpin Gel and PCR Clean-up kit. *Bam*HI (NEB, Frankfurt, Germany) was used to obtain restricted and dephosphorylated (antarctic phosphatase, NEB, Frankfurt, Germany) vector backbones, into which the gene fragments were cloned using the Gibson-Assembly method (see Supplementary material). Nucleic acid concentrations were measured with a ND-1000 spectrophotometer (Thermo Fisher Scientific, Schwerte, Germany). Transformations of $CaCl_2$ competent *E. coli* DH5α were performed via heat shock (see Supplementary material). Screening was done by colony-PCR and plasmids were isolated using the plasmid miniprep kit (GeneJET, Thermo Fisher Scientific, Schwerte, Germany). The integrity of the constructs was verified by sequencing (see Supplementary material). *C. glutamicum* cells were transformed by electroporation (see Supplementary material).

### 2.3. Genome editing by homologous recombination

Gene deletions and replacements as well as promoter exchanges were achieved via two-step homologous recombination using the suicide vector pK19*mobsacB* as previously described (see Supplementary material). Flanking regions were found using the publicly available MB001 genome (see Supplementary material). Successful genome modifications were verified by sequencing using the primers listed in the Supplementary material.

### 2.4. Fed-batch fermentation

A 3.7 L KLF bioreactor (Bioengineering AG, Wald, Switzerland) with

a working volume of 2 L, a stirrer-to-reactor diameter ratio of 0.39 and aspect ratio of 2.6:1 was used. Three Rushton turbines were installed on the central stirring axis 17, 12, and 6 cm from the bottom of the vessel. Settings for the fermentation parameters were adapted from published works on carotenoid fermentation using *C. glutamicum* (Göttl et al., 2024; Meyer et al., 2025, 2023). The temperature during the fermentation was kept at 30 °C and the pH was kept at 7 using either 100 g $L^{-1}$ phosphoric acid or 250 g $L^{-1}$ ammonia. A head space overpressure of 0.5 bar was kept throughout the process. The strain DECA(pVWEx1-*crtEBI*) was used for the fermentation, which was grown in 10 mL LB supplemented with 10 g $L^{-1}$ glucose. The second preculture, consisting of CGXII with 40 g $L^{-1}$ glucose was used to inoculate the reactor to an $OD_{600nm}$ of 1. The high-cell density medium (see Supplementary material) was used with some alterations: the trace elements were replaced by 20x concentrated CGXII trace elements and the feed consisted of 1 L of 600 g $L^{-1}$ glucose. The feed pump was primed when the relative dissolved oxygen concentration (rDOS) surpassed 60 % for the first time, indicating the consumption of the initial glucose. The addition of feed was controlled by the rDOS level, adding feed when the rDOS rose above the set threshold (initially 60 %, after 24 h lowered to 50 % and later to 45 %) Feed addition stopped when rDOS fell below 30 %, which also triggered an increase of the stirrer speed in 50 rpm steps to the maximum of 1500 rpm. Initial airflow was set to 0.25 NL $min^{-1}$ and manually increased up to 1.75 NL $min^{-1}$. Antifoam 204 was added to control foam formation. Samples were taken every 3 h by an automatic sampler and kept at 4 °C until analysis.

### 2.5. Cultivation with alternative carbon sources and orange peel hydrolysate

Cultivations on the alternative carbon sources xylose, arabinose and glycerol, as well as the orange peel hydrolysate (OPH) were carried out in the 1 mL BiolectorXT flowerplate microcultivation system (m2p-labs GmbH, Baesweiler, Germany) at 1100 rpm at 30 °C. Single carbon source cultivations were done with CGXII medium, using appropriate antibiotics and IPTG for induction of the pVWEx1 and pECXT99A plasmids. All carbon sources were concentrated as 20 g $L^{-1}$, while the set of empty vector controls for comparison with the orange peel hydrolysate were prepared on 40 g $L^{-1}$. The OPH was prepared as described in (Junker et al., 2024). There are glucose (17.8 ± 2.1 g $L^{-1}$), xylose (11.7 ± 1.2 g $L^{-1}$), arabinose (7.5 ± 0.5 g $L^{-1}$), galacturonic acid (4.2 ± 0.5 g $L^{-1}$), aspartate (0.71 ± 0.25 g $L^{-1}$), proline (0.32 ± 0.05 g $L^{-1}$), serine (0.11 ± 0.05 g $L^{-1}$) and alanine (0.09 ± 0.05 g $L^{-1}$) present in the OPH. Cultivations were carried out over the course of 48 h if not stated otherwise.

### 2.6. Carotenoid extraction and HPLC analysis

Carotenoid samples from cultures were prepared, by harvesting 0.5 mL of a culture and centrifuging it for 10 min at 21,000 x g. The cell pellet was resuspended in either a 7:3 (v $v^{-1}$) methanol:acetone mixture for standard HPLC analysis, pure methanol for the preparation of DPPH test samples, or 80 %-94 % ethanol–water solutions (adjusted for the water content of the biomass). The resuspended pellets were incubated at 60 °C for 30 min at 1000 rpm. The extract was separated from the cell debris by centrifugation at 21,000 x g for 10 min. The extraction process was repeated until the cell pellets showed no signs of residual carotenoids. For the analysis of the carotenoid extracts, an Agilent 1,200 series system (Agilent Technologies, Waldbronn, Germany), employing a C18 reverse phase column (LiChrospher 100 RP18 EC-5, 125 × 4 mm) with a pre-column (LiChrospher 100 RP18 EC-5, 40 × 4 mm). Columns were obtained from Merck KGaA (Darmstadt, Germany). A diode array detector was used to detect the carotenoids, measuring at 471 nm and recording a spectrum from 250 nm to 600 nm. Since no decaprenoxanthin standard was available, a β-carotene standard (Fisher Scientific, Schwerte, Germany) was used, hence all mass values and concentrations of decaprenoxanthin are given as β-carotene equivalents. For lycopene a standard from Carl Roth (Karlsruhe, Germany) was used. A gradient from 9:1 methanol water solution (A) to pure methanol (B) was used to separate the carotenoids at a flow rate of 1.5 mL $min^{-1}$ at the following: 0 min B: 0 %, 10 min B: 100 %, 32.5 min B: 100 %.

### 2.7. Antioxidant activity assay and stability test

To test the antioxidant activity of glucosylated and unglucosylated decaprenoxanthin, a DPPH assay was conducted. As solvent for the assay, methanol was chosen. Stock solutions of 0.2 mM DPPH, as well as 100 µg $mL^{-1}$ ascorbic acid and 100 µg $mL^{-1}$ butylated hydroxytoluene (BHT) were prepared for the assay. Decaprenoxanthin samples were obtained from pellets of WT Δ*crtR* (pVWEx1-*crtEBI*) and WT Δ*crtR* Δ*crtX* (pVWEx1-*crtEBI*) (0.5 mL culture after 48 h cultivation). Two of those pellets were each consecutively extracted with the same 1 mL methanol. The extracts of multiple pellet pairs were pooled, to obtain a stock solution of glucosylated decaprenoxanthin and unglucosylated decaprenoxanthin for the assay. The concentrations of decaprenoxanthin in the stock solutions were determined by HPLC. The extract of glucosylated decaprenoxanthin consisted of 72.1 % decaprenoxanthin diglucoside, 21.8 % decaprenoxanthin monoglucoside and 6.1 % unglucosylated decaprenoxanthin. The extract of unglucosylated decaprenoxanthin did not contain any other carotenoid than unglucosylated decaprenoxanthin. In the test, the reduction of DPPH radicals was observed spectrophotometrically at a wavelength of 517 nm, as established in the literature (see Supplementary material). In a cuvette, 500 µL of the DPPH stock solution and 500 µL of a sample solution were mixed and incubated at room temperature for 30 min in the dark. After the incubation time, the absorbance at 517 nm was measured (Seeger et al., 2023). Of the sample solutions, dilution series in 1:2 steps were prepared and tested in technical triplicates. Blanks of DPPH and the samples were prepared by diluting the respective stock solution 1:2 with methanol. With this experimental set-up, the $EC_{50}$ value of the samples was determined, meaning the concentration of an antioxidant sample in µg $mL^{-1}$ that is sufficient, to quench 50 % of the DPPH radicals in 30 min (see Supplementary material). To calculate the $EC_{50}$ values, formula 1 was first used to obtain the percentage of quenched DPPH of each reaction. The values of the sample concentrations, which were the closest above and below 50 % were then used to calculate the concentration at which 50 % of DPPH was quenched, assuming a linear behaviour in that range. The determined $EC_{50}$ values are given as means of the triplicate ± the standard deviation.

*Formula 1*

$$\frac{|[DPPHBlank]| - (|[Sample]| - |[SampleBlank]|)}{|[DPPHBlank]|} * 100 = \%quenched$$

To assess the stability of decaprenoxanthin stability tests as described in the supplementary material were conducted. The solubility of the three decaprenoxanthin species was tested as given in the supplementary material.

## 3. Results and Discussion

### 3.1. Influence of cultivation medium on decaprenoxanthin production

As a possible alternative to standard CGXII medium the previously optimized CGAST1 medium for astaxanthin production (Meyer et al., 2025) was tested regarding decaprenoxanthin production by the strains ATCC13032 Δ*crtR* (pVWEx1-*crtEBI*) and ATCC13032 Δ*crtR* Δ*crtX* (pVWEx1-*crtEBI*) overproducing glucosylated and unglucosylated decaprenoxanthin, respectively. The CGXII and CGAST1 trace salt compositions were also tested in combination with the different base media. Replacing the CGXII basis medium with the CGAST1 medium led to a significant decrease of the decaprenoxanthin titer regardless of the trace salt formulations used. This held true for both production of

glucosylated and unglucosylated decaprenoxanthin (Fig. 1A). CGAST1 and CGAST2 have been developed for astaxanthin production and increased iron, but decreased manganese concentrations improved conversion of β-carotene to astaxanthin (Meyer et al., 2025). The astaxanthin producing *C. glutamicum* differs from our decaprenoxanthin producer by the terminal reactions of carotenogenesis: lycopene via β-carotene to astaxanthin involves 3 enzymes that differ from the 2 enzyme reactions from lycopene to decaprenoxanthin (note, β-carotene is not an intermediate in the latter case). Thus, the benefit of increased iron, but decreased manganese concentrations for improved conversion

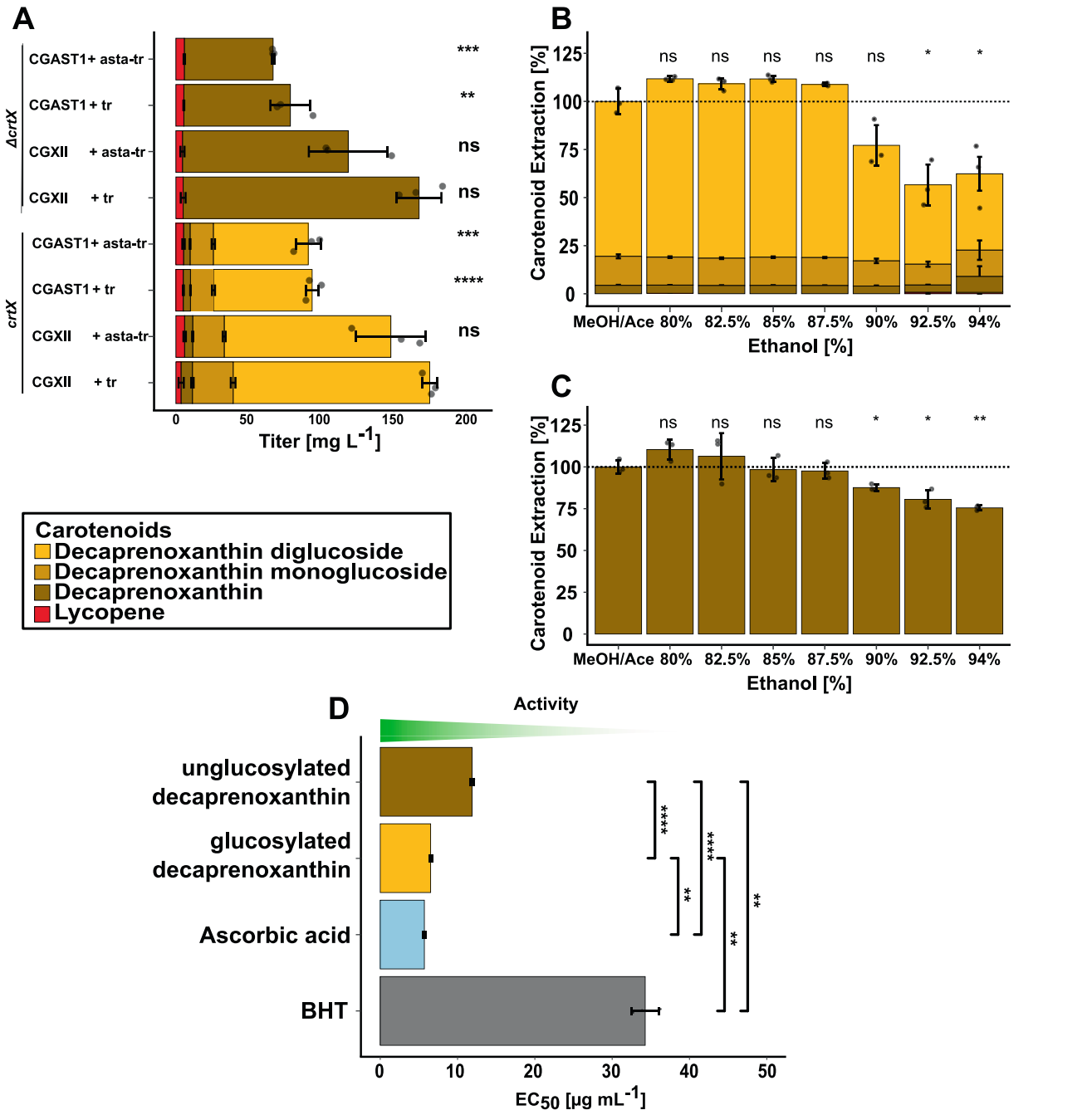


**Fig. 1. A:** Influence of media and trace salts formulations on glucosylated and unglucosylated decaprenoxanthin by strains ATCC13032 Δ*crtR* (pVWEx1-*crtEBI*) and ATCC13032 Δ*crtR* Δ*crtX* (pVWEx1-*crtEBI*). Abbreviations: tr = CGXII standard trace salts, astatr = astaxanthin optimized trace salts. Bar height indicates the mean value of the technical triplicate, error bars indicate the standard deviation, and individual total carotenoid sample values are given as dots. Statistical analysis: pair-wise t-tests (compared to the CGXII + tr with ATCC13032 Δ*crtR* (pVWEx1-*crtEBI*)). **B, C:** Decaprenoxanthin extraction efficiencies for ethanol solutions with concentrations ranging from 80 − 94 % from *C. glutamicum* biomass of a strain with intact *crtX* gene (C) and from a Δ*crtX* strain (B). The standard extraction method (MeOH/Ace) is shown for reference. Bar height indicates the mean value of the technical triplicate, error bars indicate the standard deviation, and points indicate the individual sample values. Statistical analysis: pair-wise t-tests (compared to the control). **D:** $EC_{50}$ values measured in the DPPH assay. Controls were BHT and ascorbic acid. Methanolic extracts from a strain with intact *crtX* gene ("glucosylated decaprenoxanthin"; *72.1 % decaprenoxanthin diglucoside, 21.8 % decaprenoxanthin monoglucoside and 6.1 % unglucosylated decaprenoxanthin*) and a ΔcrtX strain ("unglucosylated decaprenoxanthin"; 100 % unglucosylated decaprenoxanthin) were used. Lower $EC_{50}$ values correspond to a higher activity. Bar height indicates the mean value of the technical triplicate, error bars indicate the standard deviation, and points indicate the individual sample values. Statistical analysis: pair-wise t-tests (compared to the control). Results of statistical tests are given as significance symbols ($p < 0.05$ = *, $p < 0.01$ = **, $p < 0.001$ = ***).

of β-carotene to astaxanthin is not relevant for decaprenoxanthin production that does not involve β-carotene.

This picture is complicated by the fact that magnesium improves biomass formation and thus influences carotenoid titers. In addition, magnesium is required for decaprenoxanthin biosynthesis since CrtEb, an elongase adding the unusual C5 isoprenoid pyrophosphate (E)-4-Hydroxy-3-methyl-but-2-enyl pyrophosphate, an intermediate of the MEP pathway (Hayashi et al., 2018), to both ends of lycopene. CrtEb is absent from astaxanthin producers, but required for decaprenoxanthin production.

Thus, CGXII medium was used in the following.

### 3.2. Strain engineering increased the decaprenoxanthin titer

The strain MB001 Δ*crtR* lacking the transcriptional repressor of the carotenoid operon CrtR was used as a base strain to further exploit the decaprenoxanthin production capabilities of *C. glutamicum* since the deletion of *crtR* is known to strongly increase decaprenoxanthin accumulation by at least a factor of 10 to 30 fold (Henke et al., 2017). Three different targets were chosen along the decaprenoxanthin biosynthetic pathway. As Dxs is the rate-limiting step of the MEP pathway (Xiang et al., 2007), its native promoter was replaced by the strong constitutive promoter $P_{tuf}$ (Henke et al., 2016). Furthermore, a synthetic operon consisting of the isoprenoid pyrophosphate isomerase gene *idi* and *C. glutamicum*'s major geranylgeranyl pyrophosphate synthase (GGPPS) gene *idsA* under the promoter $P_{syn}$ was used to replace the *idi* locus (Göttl et al., 2024). Additionally, the *crt* operon was replaced with a truncated version lacking the minor GGPPS gene *crtE* and *cmpL* encoding the Corynebacterial membrane protein Large transporter and expressed under the control of the $P_{tac}$ promoter. No significant differences in growth behaviour were found upon genomic modifications (Fig. S1). Taken individually, only the *dxs* promoter exchange led to a significantly increased decaprenoxanthin titer (Fig. 2A). Decaprenoxanthin could be improved when the precursor supply (GGPP) was increased, *i.e.*, by substituting *dxs* promoter and overexpressing *idsA* and *idi.* Overexpression of the *crtBIYefEb* operon did not improve decaprenoxanthin, indicating that the conversion of GGPP to decaprenoxanthin is not a metabolic bottleneck (at least until decaprenoxanthin levels reached here). However, the combination of the *dxs* promoter exchange and the $P_{syn}$-*idsA-idi* integration further increased the titer, while the strain harbouring all three integrations yielded the highest observed titer, being significantly higher than all other strains except for *idi*::$P_{syn}$-*idsA-idi dxs*::$P_{tuf}$-*dxs,* with 127.6 ± 14.5 mg $L^{-1}$ of total carotenoids (Fig. 2A). The triple integrant (*ΔcrtOperon*::$P_{tac}$-*crtBIY*$_{ef}$*Eb idi*::$P_{syn}$-*idsA-idi dxs*::$P_{tuf}$-*dxs.*) was named strain DECA and used in the following.

Plasmid-based gene overexpression was tested in addition to genome editing. First, *dxs* either from *C. glutamicum* or the related *Corynebacterium efficiens* (Li et al., 2021) were overexpressed from plasmid pVWEx1. In addition and independently, the *crtBIY*$_{ef}$*Eb* operon from *C. efficiens* was expressed from the plasmid pECXT-$P_{syn}$. However, no beneficial effect on decaprenoxanthin production was observed (Fig. S2) although this strategy increased α-carotene production by *C. glutamicum* (Li et al., 2021). Thus, plasmid-born expression of *dxs* and of *crt* genes from *C. efficiens* in addition to the genome modifications of strain DECA did not improve decaprenoxanthin titers.

Next, we compared plasmid-born overexpression of operons with the native genes *crtE* (encoding the minor GGPPS), *crtB* (encoding phytoene synthase) and *crtI* (encoding phytoene desaturase) or just *crtB* and *crtI*. Increases in decaprenoxanthin titers were present in the strains harbouring pVWEx1-*crtEBI* as well as pECXT-$P_{syn}$-*crtBI*. These strains did not significantly differ from each other, with the pVWEx1-*crtEBI* strain achieving a titer of 229.6 ± 6.0 mg $L^{-1}$ and the pECXT-$P_{syn}$-*crtBI* strain reaching a titer of 193.3 ± 29.0 mg $L^{-1}$ (Fig. 2B and Fig. S6). Since the pVWEx1-*crtEBI* carrying strain showed the highest decaprenoxanthin production, we continued with *C. glutamicum* DECA(pVWEx1-*crtEBI*) in the following.

### 3.3. Overexpression of crtX increased decaprenoxanthin glucosylation

All decaprenoxanthin producing strains showed different ratios of unglucosylated, monoglucosylated and diglucosylated decaprenoxanthin. In addition, the glucosylation status may depend on cultivation conditions or the growth phase. Deletion of the native glucosyltransferase gene *crtX* is known to result in production of only unglucosylated decaprenoxanthin (Heider et al., 2014a). Here, we tested if *crtX* overexpression increased the glucosylation status of decaprenoxanthin. Plasmid pEKEx3 containing either the native *crtX* or a homolog from *Pantoea ananatis*, which codes for a C40 specific glucosyl-transferase, was used to transform strain DECA(pVWEx1-*crtEBI*). The growth rates in these strains carrying two plasmids were lower than in the single plasmid strain, while this effect was more pronounced for the strain overexpressing the *crtX* from *C. glutamicum* (Fig. S7). Decaprenoxanthin production was lower than by the parental strains or the empty vector carrying strain. The strain overexpressing *crtX* from *P. ananatis* accumulated 93.5 ± 4.9 mg $L^{-1}$, of which 80 % was diglucosylated. The strain overexpressing the native *crtX* from *C. glutamicum* accumulated 121.6 ± 11.3 mg $L^{-1}$ decaprenoxanthin, 90 % of which was diglucosylated decaprenoxanthin, both of which produced significantly less than the controls (Fig. 2C). Thus, while complete diglucosylation of decaprenoxanthin was not observed and overexpression of both *crtX* variants reduced the total decaprenoxanthin titer, strain DECA(pVWEx1-*crtEBI*) (pEKEx3-*crtX*(Cg)) was the best strain for production of diglucosylated decaprenoxanthin.

The glucosylation status of decaprenoxanthin was varied as glucosylation may exert a metabolic pull. As described earlier (Heider et al., 2014a), deletion of *crtX* abolished glucosylation of decaprenoxanthin, thus, the unglucosylated decaprenoxanthin can be obtained in a pure form. Likewise, but incomplete, overexpression of *crtX* increased decaprenoxanthin glucosylation yielding diglucosylated decaprenoxanthin as major product (up to 90 %). While CrtX from *C. glutamicum* glucosylated decaprenoxanthin. sarcinaxanthin, and C.p.450, but was not active with the C40 carotenoid zeaxanthin, CrtX from *P. ananatis* did not only glucosylate zeaxanthin, but also decaprenoxanthin (Heider et al., 2014a). Glucosylation was not complete as also observed for CrtX from *P. ananatis* or *Fulvimarina pelagi* regarding astaxanthin glucosylation in *C. glutamicum* (Göttl et al., 2024). Currently, it is not known what limits decaprenoxanthin glucosylation (*i.a.*, gene expression or the UDP-glucose pool size). The fed-batch bioreactor cultivation led to higher decaprenoxanthin glucosylation than shake flask cultivation as did the use of orange peel hydrolysate compared to mineral salts medium. CrtX uses UDP-glucose as substrate for the glucosylation of decaprenoxanthin. The availability of UDP-glucose may be better in the bioreactor and in the orange peel hydrolysate, enabling the observed glucosylation increase. Overexpression of *crtX* increases the UDP-glucose requirements which in turn may reduce the availability of carotenogenesis precursors such as pyruvate or glyceraldehyde 3-phosphate, the precursors of the MEP pathway. Future metabolomic and carbon flux experiments will be required to test this hypothesis though. As CrtX of *C. glutamicum* is also able to glucosylate sarcinaxanthin and C.p.450 and deletion of *crtX* abrogated their glucosylation (Heider et al., 2014a), it is likely that these compounds may be obtained with high glucosylation status by the procedures described here.

### 3.4. Scale-up to 2 L fed-batch bioreactor cultivation

To test if the production is stable in a bench-top stirred bioreactor, a 2 L fed-batch fermentation was performed. The strain DECA(pVWEx1-*crtEBI*) was transferred to a high-cell density fed-batch fermentation, which was carried out in a similar manner as other carotenoid fermentations (Göttl et al., 2024; Meyer et al., 2025, 2023) with detailed parameters given in the methods section. The feed program was started after 5 h and the consumption of the initial glucose supply as indicated by the rDOS peak around that time. The feed was finished after 69 h,

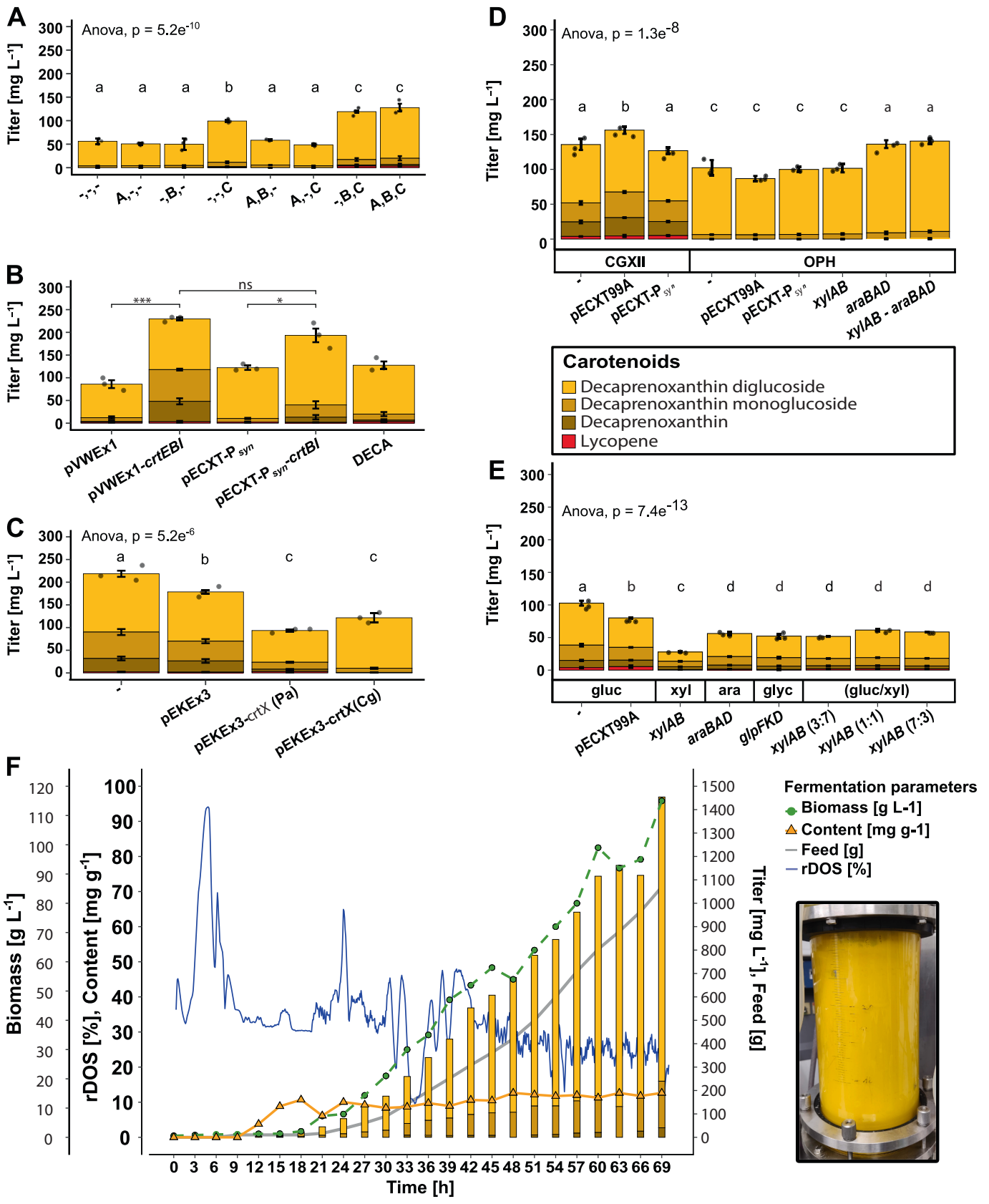


*(caption on next page)*

**Fig. 2. A, B, C:** Carotenoid production of the MB001 Δ*crtR* based integration strains (A), plasmid based *crtBI / crtEBI* overexpression (B), and additional overexpression of *crtX* (Cg = *C. glutamicum*, Pa=*P. ananatis*) (C). Bar height indicates the mean value of the technical triplicate, error bars indicate the standard deviation, and individual total carotenoid sample values are given as dots. In figure A, integrations are abbreviated as A: *ΔcrtOperon*::$P_{tac}$-*crtBIY$_{ef}$Eb*, B: *idi*::$P_{syn}$-*idsA-idi*, C: *dxs*::$P_{tuf}$-*dxs*. Statistical analysis: (A, C) Anova + post-hoc *t*-test, (B) pair-wise t-tests (compared to the control). **D, E:** Decaprenoxanthin titers from 1 mL BioLector cultivations on xylose (xyl), arabinose (ara), glycerol (glyc) and glucose xylose mixtures (gluc/xyl)(F and G). All carbon sources were provided as 20 g $L^{-1}$. The orange peel hydrolysate was used as 80:20 mixture with a 1 M phosphate buffer, while the CGXII cultivations in this case were done with 40 g $L^{-1}$. Carotenoid are given as titer in mg $L^{-1}$. The genes expressed with the pECXT99A or pECXT-$P_{syn}$ in the case of *xylAB-araBAD* ("- "= no plasmid, "pECXT99A", "pECXT-$P_{syn}$" =empty vector) and the carbon sources are given on the x-axis. Bar height indicates the mean value of the technical triplicate, error bars indicate the standard deviation, and individual total carotenoid sample values are given as dots. Statistical analysis: Anova + post-hoc *t*-test. **F:** Fed-batch fermentation with DECA (pVWEx1-*crtEBI*). Carotenoid titers are given as bars, biomass is given as green circles, the carotenoid content per biomass (mg $g^{-1}$) is given in orange triangles, the cumulatively added feed is given as grey line, and the relative dissolved oxygen saturation (rDOS) as blue line. A picture of the fermenter is shown in the inlet. Results of Anova + post-hoc t-tests are given as group labels in the bars, Anova p-value is given in each subfigure. Results of pair-wise t-tests are given as significance symbols ($p < 0.05$ = *, $p < 0.01$ = **). (For interpretation of the references to colour in this figure legend, the reader is referred to the web version of this article.)

when about 115 g $L^{-1}$ of biomass had accumulated and about 1450 mg $L^{-1}$ of total decaprenoxanthin had been produced. Notably, about 83 % of the produced decaprenoxanthin was diglucosylated. The process showed a volumetric production rate of 21 mg $L^{-1}$ $h^{-1}$, a substrate specific product yield $Y_{PS}$ of 4.8 mg $g^{-1}$ and a biomass specific product yield $Y_{PX}$ of 12.6 mg $g^{-1}$, which remained stable throughout the process (Fig. 2F).

*C. glutamicum* is best known for the industrial production of amino acids and other nitrogenous compounds that are secreted out of the cell. The coproduction of secreted amino acids and cell-bound carotenoids has been established for *C. glutamicum* (Henke et al., 2018). To maximize carotenoid production *C. glutamicum* has to be engineered such that only one major product, here decaprenoxanthin, is synthesized. This work was based on the knowledge that *Corynebacteria* natively synthesize small amounts of decaprenoxanthin, in the case of *C. glutamicum* in a diglucosylated form (Krubasik et al., 2001). In this work, a decaprenoxanthin producer strain has been engineered that is capable of producing 230 mg $L^{-1}$ in shake flask cultures and 1450 mg $L^{-1}$ of decaprenoxanthin in a 2 L fed-batch setting. In general this represents one of the highest carotenoid titers achieved by *C. glutamicum* so far, as gram-*per*-liter-scale production has only been described for α-carotene (Li et al., 2024) and lutein (Eun et al., 2025). It must be noted that the given titers represent decaprenoxanthin in terms of β-carotene equivalents, since no decaprenoxanthin standards are commercially available. The resulting systemic error is in this case not easily estimated, given the difference in molecular mass and spectral specifications between decaprenoxanthin and β-carotene. Decaprenoxanthin production may benefit from further metabolic engineering approaches, e.g., modifications of the carbon and energy metabolism according to target identification by CRISPRi screening (Göttl et al., 2021), integration of multiple *crt* gene copies, implementation of MVA pathway in addition to the MEP pathway or as substitution (Li et al., 2021; Luckie et al., 2024; Sasaki et al., 2019).

The decaprenoxanthin titer achieved here is to the best of our knowledge the highest described for a C50 carotenoid. By comparison, halophilic bacteria like *Halorubrum ruber*, *Haloferax marinum,* and *Haloferax mediterrane* produced titers of 556 mg $L^{-1}$, 2.2 mg $L^{-1}$, and 2 mg $L^{-1}$ respectively (Chen et al., 2015; Cho et al., 2024; Hwang et al., 2024). Furthermore, 0.7 mg $L^{-1}$ bacterioruberin was produced on methane using microbial consortia (Guo et al., 2024). Recently, the production of 9.7 mg $L^{-1}$ bacterioruberin has been described for *C. glutamicum* (Cho et al., 2025). Besides these linear C50 carotenoids, *C. glutamicum* has been engineered produce the cyclic C50 carotenoids sarcinaxanthin and C.p.450 (Heider et al., 2014a; Netzer et al., 2010).

### 3.5. Decaprenoxanthin production on alternative carbon sources and orange peel hydrolysate

Access to alternative carbon sources that do not have competing uses in food and feed is desirable for sustainable biotechnological processes. Previously, the utilization of the alternative carbon sources xylose and arabinose (pentose sugars present in lignocellulosic hydrolysates) or glycerol (a stoichiometric by-product from the biodiesel process) has been enabled by metabolic engineering of *C. glutamicum* (Zahoor et al., 2012). Here, strain DECA(pVWEx1-*crtEBI*) was engineered for heterologous expression of the respective genes *xylAB*, *araBAD*, and *glpFKD* based on the plasmid pECXT99A. The strains were cultivated in CGXII medium with 20 g $L^{-1}$ of the respective carbon source for 96 h. The xylose utilizing strain grew to the lowest $OD_{600nm}$ of 7.0 ± 0.5 with all other conditions reaching values between 16 and 26. The biomass specific yield was comparable for all strains and conditions. All strains accumulated decaprenoxanthin (Fig. 2E and Fig. S15B) although decaprenoxanthin titers and glucosylation ratios varied moderately, with significant difference in the titer showing between the alternative carbon conditions and the controls.

Next, we tested orange peel hydrolysate (Junker et al., 2024), a real-world food waste, as substrate for decaprenoxanthin production. Cultivating the *xylAB* or *araBAD* expressing strains, as well as a strain carrying plasmid pECXT-$P_{syn}$-*xylAB-araBAD* on orange peel hydrolysate resulted in titers of 102.3 ± 10.7 mg $L^{-1}$ of total carotenoid in the basis strain and 136.1 ± 7.3 mg $L^{-1}$ and 140.5 ± 5.0 mg $L^{-1}$ for the strains expressing *araBAD* and the *xylAB-araBAD* combination respectively (Fig. 2D). These strains achieved the highest titers on the OPH and fared comparable (no significant difference) to the CGXII control of the basis strain and the pECXT-$P_{syn}$ empty vector control on glucose CGXII (135.6 ± 12.1 mg $L^{-1}$ and 126.8 ± 6.1 g $L^{-1}$). The utilization of orange peel hydrolysate as substrate resulted in more diglucosylated decaprenoxanthin in comparison to the CGXII controls, both in relation to the other decaprenoxanthin species and regarding total titers. In this case, the *xylAB-araBAD* strain produced diglucosylated decaprenoxanthin to the highest titer (129.6 ± 3.5 mg $L^{-1}$), making up 92 % of the total carotenoid produced by this strain. The carotenoid contents on orange peel hydrolysate were similar to the basis strain harbouring the pECXT-$P_{syn}$ empty vector control and only significantly lower than the pECXT99A empty vector control (Fig. S15A).

A flexible feedstock concept has been realized for *C. glutamicum* to utilise alternative carbon sources such as glycerol, arabinose, and xylose (Zahoor et al., 2012), as well as side streams from aquaculture (Schmitt et al., 2023), from starch production (Burgardt et al., 2021) or from orange peel (Junker et al., 2024). The applications described so far mostly targeted production of secreted compounds from alternative feedstocks, while here a cell-bound carotenoid was produced. Purification of secreted products such as amino acids (Junker et al., 2024) is impacted more by seasonal and geographical variation than production of cell-bound products. Purification of secreted products may need additional steps to separate products from residual components since hydrolysates of side streams are complex and are not utilized completely. By contrast, the purification procedure by cell harvesting and extraction is likely very similar for cell-bound products when produced either from pure substrates in a mineral salt medium or from a complex hydrolysate. While glucose is the mainly used carbon source in this work, we provided some examples of alternative carbon sources and a food waste side stream being used in place of glucose. Titers obtained by fermentation from pentose sugars, glycerol or hydrolysates are

typically lower than from glucose in mineral salts media as was observed here as well. However, the product on biomass yields ($Y_{PX}$) were similar for all tested conditions while maximal biomass concentrations varied with the substrate. Xylose utilization was shown to be beneficial for the production of the C40 carotenoid α-carotene (Li et al., 2024) which in this case may have been due to the presence of both the MEP and MVA pathways.

Orange peel hydrolysate supported growth and production of, e.g., tyrosine well without further engineering of alternative substrate utilization (Junker et al., 2024). Here, plasmid-based expression of the genes *araBAD* and *xylAB* enabled the decaprenoxanthin producer strain to utilize arabinose and xylose from the hydrolysate, increasing the resulting product titers. Thus, this strategy may help to boost further processes based on hydrolysates of orange peel or similar agriculture side-streams, though this will need further rigorous work to firmly establish this mode of production. The properties of the used hydrolysate may vary with seasonal effects and the processing of the oranges, which may influence the success of a fermentation, but also carries implications for the downstream processing of the yielded product. Moreover, it is noteworthy that cultivation on the orange peel hydrolysate led to a higher share of diglucosylated decaprenoxanthin, showing an advantage of orange peel hydrolysate over the usual CGXII medium regarding the glucosylation status of decaprenoxanthin although the underlying mechanism remains unclear.

### 3.6. Glucosylated decaprenoxanthin shows a higher antioxidative activity and degradation under UV light

Antioxidants are important active ingredients for the cosmetics industry (Kusumawati and Indrayanto, 2013). Therefore, the antioxidative activity of decaprenoxanthin was tested using an *in vitro* DPPH assay. Methanolic extracts from either the *ΔcrtR* (pVWEx1-*crtEBI*) strain or the *ΔcrtR ΔcrtX* (pVWEx1-*crtEBI*) strain were used to examine "glucosylated decaprenoxanthin" and "unglucosylated decaprenoxanthin", respectively (Fig. 1D).

The results are given as the half-maximal effective concentration ($EC_{50}$), with lower values corresponding to a higher activity. Hereby, both decaprenoxanthin samples showed a significantly higher activity than the BHT control. Compared to each other, the sample with unglucosylated decaprenoxanthin showed a lower activity ($EC_{50}$ of 11.9 ± 0.2 μg $mL^{-1}$) than the glucosylated sample ($EC_{50}$ of 6.5 ± 0.2 μg $mL^{-1}$), which is comparable to that of vitamin C ($EC_{50}$ of 5.8 ± 0.2 μg $mL^{-1}$ for ascorbate).

Concerning the stability of decaprenoxanthin under UV-A light, we found that after 6 h of exposure, no detectable amounts of decaprenoxanthin or diglucosylated decaprenoxanthin were left, with concentrations halved after about 2 h, while the controls did not show substantial decreases (Fig. S11). However, for the heat-treated samples at 90 °C, the concentrations did not drop below 70 % of the initial concentration after 6 h of incubation (Fig. S12). At 60 °C the concentration of glucosylated decaprenoxanthin dropped to about 85 % after 6 h, while the unglycosylated samples showed slight relative increases.

Glucosylation of decaprenoxanthin was found to lead to an increased antioxidative activity in a DPPH assay. An increase of the antioxidative activity of carotenoids upon glucosylation has been reported in other cases as well, though the mechanism by which the glycosylation aids the antioxidative activity is still unclear (Sandmann, 2019). While the glucose moiety is neither connected to, nor in the proximity of the conjugated double bond system, which is responsible for the radical quenching capabilities, nor is itself an antioxidant, glucosylation affects solubility in aqueous systems, which may affect antioxidative activity as measured in the DPPH assay. The near doubling of the antioxidative activity in the glucosylated extract brought its activity close to that of ascorbic acid/vitamin C ($EC_{50}$ values of 6.5 ± 0.2 μg $mL^{-1}$ and 5.8 ± 0.2 μg $mL^{-1}$). The reported $EC_{50}$ values for decaprenoxanthin are as of now the first published values for this carotenoid. For comparison, $EC_{50}$ values with the DPPH assay have been determined for the C50 carotenoid bacterioruberin (2.22 μg $mL^{-1}$ and 160 μg $mL^{-1}$ depending on the *Haloferax* species used for extraction (Alvares and Furtado, 2021) or for β-carotene ($EC_{50}$ value of 63.9 μg $mL^{-1}$ (Rohmah et al., 2022). Notably, although less active than *C. glutamicum*-derived astaxanthin ($EC_{50}$ value of 4.5 μg $mL^{-1}$), decaprenoxanthin showed higher antioxidant power than chemically synthesised astaxanthin (41.9 μg $mL^{-1}$) (Seeger et al., 2023). An important structural feature for the antioxidative activity is the conjugated double bond system, the length of which correlates with the antioxidative activity (Di Mascio et al., 1991). Even though decaprenoxanthin only possess 9 conjugated double bonds (4 additional unconjugated double bonds), it does fare better than some carotenoids with larger double bond systems, as given by the available literature. It is likely that such differences are caused by the extraction methods and handling of the samples in those studies, rather than by an intrinsic property of decaprenoxanthin. Though it still suggests that the methods for extraction used here keep the decaprenoxanthin in a highly active condition. Factors that undermine the integrity of carotenoids are light exposure and heat (Chen et al., 1996). Here we tested the stability of decaprenoxanthin at 60 °C and 90 °C for up to 6 h and found decaprenoxanthin to be stable at 60 °C for at least 1 h. Since our used extraction method uses 60 °C as incubation temperature for 30 min, this is a reassuring finding. Stability under light exposure was tested with UV-A light, a harmful wavelength range against which decaprenoxanthin is considered to be a photo protectant and patented as sunscreen ingredient (Goksøyr, 2013). It rapidly degrades under UV-A light, with no detectable amounts left after 6 h. The glucosylation did in this case not impact the stability, with both glucosylated and unglycosylated decaprenoxanthin degrading in a similar fashion. The spectral attributes of decaprenoxanthin are not impacted by glucosylation (see Fig. S13 and Fig. S14), explaining why the glucosylation does not impact the stability against UV-A radiation.

### 3.7. Ethanol as a green solvent for decaprenoxanthin extraction

In this study, decaprenoxanthin has been extracted with a methanol: acetone mixture for quantification and with methanol for the DPPH assay. However, these routine procedures are not valid for application in the cosmetic industry as here non-harmful solvents are desired. Ethanol, which is a generally recognized as safe (GRAS) solvent (Addo et al., 2022), has been shown to efficiently extract biomass-bound astaxanthin from *C. glutamicum* (Seeger et al., 2023). In a similar approach, the applicability of ethanol as extraction solvent for glucosylated and unglucosylated decaprenoxanthin extractions was tested.

Considering the humidity of the biomass, ethanol–water solutions ranging from 80 % to 94 % ethanol in 2.5 % steps were tested and compared to the standard method using a 7:3 mixture of methanol and acetone. The extractions were done with biomass from the *ΔcrtR* (pVWEx1-*crtEBI*) strain for "unglucosylated decaprenoxanthin" and the *ΔcrtR ΔcrtX*(pVWEx1-*crtEBI*) strain for "glucosylated decaprenoxanthin". In both cases, ethanol concentrations of 90 % and higher extracted significantly less decaprenoxanthin, while lower concentrations did not significantly differ from the control (Fig. 1B and C). Thus, it can be concluded that ethanol concentrations between 80 % and 90 % serve as an efficient green extraction process for decaprenoxanthin from corynebacterial biomass.

Just as astaxanthin, decaprenoxanthin can be directly extracted with the green solvent ethanol without previous physical treatments, at a similar efficiency as with methanol, enabling use cases in which the use of methanol is prohibited or tightly regulated (Tekin et al., 2018). The extraction efficiency did not depend on the glucosylation state of the decaprenoxanthin, although a qualitative difference in water solubility was observed when estimating the log $P_{OW}$ values for the decaprenoxanthin species (Fig. S9). In addition to ethanol, supercritical carbon dioxide extraction might be another green extraction method for decaprenoxanthin as this was recently established for the extraction of

astaxanthin from *C. glutamicum* (Seeger et al., 2025).

## 4. Conclusion

In this work, a decaprenoxanthin producer strain, achieving a g $L^{-1}$ titer in a 2 L fed-batch fermentation has been constructed. We report the first measurements of the antioxidative activity of decaprenoxanthin in a DPPH assay and the impact of its glucosylation state on said activity and the solubility. With the constructed strain as basis, a C50 platform strain could be build, likely enabling the production of other C50 carotenoids and their glucosides, also with the potential of g $L^{-1}$ titers. While this can be done using glucose containing medium, we also showed that orange peel hydrolysate can be used as sustainable alternative. Combined these can give the opportunity for a side stream utilizing production of a patented sunscreen ingredient and antioxidant, which can also be extracted from the biomass in an environmentally friendly and health hazard reduced way with the use of ethanol.

## CRediT authorship contribution statement

**Fynn Stegelmann:** Writing – review & editing, Writing – original draft, Methodology, Formal analysis, Data curation. **Jan Seeger:** Writing – review & editing, Writing – original draft, Methodology, Formal analysis, Data curation. **Petra Peters-Wendisch:** Writing – review & editing, Methodology, Formal analysis. **Nadja A. Henke:** Writing – review & editing, Methodology, Funding acquisition, Formal analysis, Conceptualization. **Volker F. Wendisch:** Writing – review & editing, Supervision, Methodology, Funding acquisition, Formal analysis, Data curation, Conceptualization.

## Declaration of competing interest

The authors declare the following financial interests/personal relationships which may be considered as potential competing interests: Nadja A. Henke reports financial support was provided by Bielefeld University. If there are other authors, they declare that they have no known competing financial interests or personal relationships that could have appeared to influence the work reported in this paper.

## Acknowledgements

The authors thank Irene Krahn for cloning the pECXT99A-*glpFKD* vector and Dr. Ina Schmitt and Dr. Vanessa Göttl for support during project initiation. This work was supported in part by the German Federal Ministry of Education and Research (BMBF) project KaroTec (grant number: 03VP09460).

## Appendix A. Supplementary data

Supplementary data to this article can be found online at https://doi.org/10.1016/j.biortech.2025.133319.

## Data availability

Data will be made available on request.

## References

Addo, P.W., Sagili, S.U., Bilodeau, S.E., Gladu-Gallant, F.-A., MacKenzie, D.A., Bates, J., McRae, G., MacPherson, S., Paris, M., Raghavan, V., Orsat, V., Lefsrud, M., 2022. Cold Ethanol Extraction of Cannabinoids and Terpenes from Cannabis Using Response Surface Methodology: Optimization and Comparative Study. Molecules 27, 8780. https://doi.org/10.3390/molecules27248780.

Alvares, J., Furtado, I., 2021. Kinetics of DPPH• scavenging by bacterioruberin from *Haloferax alexandrinus* GUSF-1 (KF796625). J. Anal. Sci. Technol. 12, 44. https://doi.org/10.1186/s40543-021-00293-3.

Andrewes, A.G., Liaaen-Jensen, S., 1984. REVISION OF THE STRUCTURES OF THE BACTERIAL C50-CAROTENOIDS C.P. 450 and C.P.473. Tetrahedron. Lett. 25, 1191–1194. https://doi.org/10.1016/S0040-4039(01)91557-6.

Bin-Jumah, M., Alwakeel, S.S., Moga, M., Buvnariu, L., Bigiu, N., Zia-Ul-Haq, M., 2021. Application of Carotenoids in Cosmetics. In: Zia-Ul-Haq, M., Dewanjee, S., Riaz, M. (Eds.), Carotenoids: Structure and Function in the Human Body. Springer, Cham. https://doi.org/10.1007/978-3-030-46459-2_24.

Burgardt, A., Prell, C., Wendisch, V.F., 2021. Utilization of a Wheat Sidestream for 5-Aminovalerate Production in *Corynebacterium glutamicum*. Front. Bioeng. Biotechnol. 9, 732271. https://doi.org/10.3389/fbioe.2021.732271.

Chen, C.W., Hsu, S., hui, Lin, M.T., Hsu, Y. Hui, 2015. Mass production of C50 carotenoids by *Haloferax mediterranei* in using extruded rice bran and starch under optimal conductivity of brined medium. Bioprocess. Biosyst. Eng. 38, 2361–2367. https://doi.org/10.1007/s00449-015-1471-y.

Chen, H.E., Peng, H.Y., Chen, B.H., 1996. Stability of carotenoids and vitamin A during storage of carrot juice. Food Chem 4, 497–503.doi. https://doi.org/10.1016/S0308-8146(96)00008-8.

Cho, E.-S., Hwang, C.Y., Seo, M.-J., 2025. Enhanced production of C50 carotenoid bacterioruberin by metabolically engineered *Corynebacterium glutamicum*. Bioresour. Technol. 432, 132670. https://doi.org/10.1016/j.biortech.2025.132670.

Cho, E.S., Hwang, C.Y., Seo, M.J., 2024. Optimized production of bacterioruberin from "*Haloferax marinum*" using one-factor-at-a-time and central composite design approaches. Bioresour. Bioproc. 11, 111. https://doi.org/10.1186/s40643-024-00834-9.

Di Mascio, P., Murphy, M., Sies, H., 1991. Antioxidant defense systems: the role of carotenoids, tocopherols, and thiols. Am. J. Clin. Nutr. 53, 194S–200S. https://doi.org/10.1093/ajcn/53.1.194S.

Eun, H., Prabowo, C.P.S., Lee, S.Y., 2025. Gram-per-litre-scale production of lutein by engineered *Corynebacterium*. Nat. Synth. https://doi.org/10.1038/s44160-025-00826-3.

Goksøyr, A., 2013. Carotenoid sunscreen. WO2011151426A2.

Göttl, V.L., Meyer, F., Schmitt, I., Persicke, M., Peters-Wendisch, P., Wendisch, V.F., Henke, N.A., 2024. Enhancing astaxanthin biosynthesis and pathway expansion towards glycosylated C40 carotenoids by *Corynebacterium glutamicum*. Sci. Rep. 14, 8081. https://doi.org/10.1038/s41598-024-58700-9.

Göttl, V.L., Schmitt, I., Braun, K., Peters-Wendisch, P., Wendisch, V.F., Henke, N.A., 2021. CRISPRi-Library-Guided Target Identification for Engineering Carotenoid Production by *Corynebacterium glutamicum*. Microorganisms 9, 670. https://doi.org/10.3390/microorganisms9040670.

Grung, M., D'Souza, F.M.L., Borowitzka, M., Liaaen-Jensen, S., 1992. Algal Carotenoids 51. Secondary carotenoids 2. *Haematococcus pluvialis* aplanospores as a source of (3S, 3′S)-astaxanthin esters. J. Appl. Phycol. 4, 165–171. https://doi.org/10.1007/BF02442465.

Guo, S., Song, Q., Song, X., Zhang, C., Fei, Q., 2024. Sustainable production of C50 carotenoid bacterioruberin from methane using soil-enriched microbial consortia. Bioresour. Technol. 412, 131415. https://doi.org/10.1016/j.biortech.2024.131415.

Hayashi, Y., Ito, T., Yoshimura, T., Hemmi, H., 2018. Utilization of an intermediate of the methylerythritol phosphate pathway, (E)-4-hydroxy-3-methylbut-2-en-1-yl diphosphate, as the prenyl donor substrate for various prenyltransferases. Biosci. Biotechnol. Biochem. 82, 993–1002. https://doi.org/10.1080/09168451.2017.1398064.

Heider, S.A.E., Peters-Wendisch, P., Netzer, R., Stafnes, M., Brautaset, T., Wendisch, V.F., 2014a. Production and glucosylation of C50 and C40 carotenoids by metabolically engineered *Corynebacterium glutamicum*. Appl Microbiol. Biotechnol. 98, 1223–1235. https://doi.org/10.1007/s00253-013-5359-y.

Heider, S.A.E., Peters-Wendisch, P., Wendisch, V.F., 2012. Carotenoid biosynthesis and overproduction in *Corynebacterium glutamicum*. BMC Microbiology 12, 198. https://doi.org/10.1186/1471-2180-12-198.

Heider, S.A.E., Wolf, N., Hofemeier, A., Peters-Wendisch, P., Wendisch, V.F., 2014b. Optimization of the IPP precursor supply for the production of lycopene, decaprenoxanthin and astaxanthin by *Corynebacterium glutamicum*. Front. Bioeng. Biotechnol. 2, 28. https://doi.org/10.3389/fbioe.2014.00028.

Henke, N.A., Heider, S.A.E., Hannibal, S., Wendisch, V.F., Peters-Wendisch, P., 2017. Isoprenoid pyrophosphate-dependent transcriptional regulation of carotenogenesis in *Corynebacterium glutamicum*. Front. Microbiol. 8, 633. https://doi.org/10.3389/fmicb.2017.00633.

Henke, N.A., Heider, S.A.E., Peters-Wendisch, P., Wendisch, V.F., 2016. Production of the marine carotenoid astaxanthin by metabolically engineered *Corynebacterium glutamicum*. Mar. Drugs 14, 124. https://doi.org/10.3390/md14070124.

Henke, N.A., Wiebe, D., Pérez-García, F., Peters-Wendisch, P., Wendisch, V.F., 2018. Coproduction of cell-bound and secreted value-added compounds: Simultaneous production of carotenoids and amino acids by *Corynebacterium glutamicum*. Bioresour. Technol. 247, 744–752. https://doi.org/10.1016/j.biortech.2017.09.167.

Hwang, C.Y., Cho, E.-S., Kim, S., Kim, K., Seo, M.-J., 2024. Optimization of bacterioruberin production from *Halorubrum ruber* and assessment of its antioxidant potential. Microb Cell Fact 23, 2. https://doi.org/10.1186/s12934-023-02274-0.

Junker, N., Sariyar Akbulut, B., Wendisch, V.F., 2024. Utilization of orange peel waste for sustainable amino acid production by *Corynebacterium glutamicum*. Front. Bioeng. Biotechnol. 12, 1419444. https://doi.org/10.3389/fbioe.2024.1419444.

Krubasik, P., Takaichi, S., Maoka, T., Kobayashi, M., Masamoto, K., Sandmann, G., 2001. Detailed biosynthetic pathway to decaprenoxanthin diglucoside in *Corynebacterium glutamicum* and identification of novel intermediates. Arch. Microbiol. 176, 217–223. https://doi.org/10.1007/s002030100315.

Kusumawati, I., Indrayanto, G., 2013. Chapter 15 - Natural Antioxidants in Cosmetics, in: Atta-ur-Rahman, F.R.S. (Ed.), Studies in Natural Products Chemistry. Elsevier, pp. 485–505. https://doi.org/10.1016/B978-0-444-59603-1.00015-1.

Li, C., Swofford, C.A., Rückert, C., Chatzivasileiou, A.O., Ou, R.W., Opdensteinen, P., Luttermann, T., Zhou, K., Stephanopoulos, G., Prather, K.L.J., Zhong-Johnson, E.Z.L., Liang, S., Zheng, S., Lin, Y., Sinskey, A.J., 2021. Heterologous production of α-carotene in *Corynebacterium glutamicum* using a multi-copy chromosomal integration method. Bioresour. Technol. 341, 125782. https://doi.org/10.1016/j.biortech.2021.125782.

Li, K., Li, C., Liu, C.G., Zhao, X.Q., Ou, R., Swofford, C.A., Bai, F.W., Stephanopoulos, G., Sinskey, A.J., 2024. Engineering carbon source division of labor for efficient α-carotene production in *Corynebacterium glutamicum*. Metab. Eng. 84, 117–127. https://doi.org/10.1016/j.ymben.2024.06.008.

Luckie, B.A., Kashyap, M., Pearson, A.N., Chen, Y., Liu, Y., Valencia, L.E., Romero, A.C., Hudson, G.A., Tao, X.B., Wu, B., Petzold, C.J., Keasling, J.D., 2024. Development of *Corynebacterium glutamicum* as a monoterpene production platform. Metab. Eng. 81, 110–122. https://doi.org/10.1016/j.ymben.2023.11.009.

Meyer, F., Schmitt, I., Schäffer, T., Wendisch, V.F., Henke, N.A., 2023. Design-of-Experiment-Guided Establishment of a Fermentative Bioprocess for Biomass-Bound Astaxanthin with *Corynebacterium glutamicum*. Fermentation 9, 969. https://doi.org/10.3390/fermentation9110969.

Meyer, F., Schmitt, I., Wendisch, V.F., Henke, N.A., 2025. Response surface-based media optimization for astaxanthin production in *Corynebacterium glutamicum*. Front. Bioeng. Biotechnol. 13, 151652. https://doi.org/10.3389/fbioe.2025.1516522.

Netzer, R., Stafsnes, M.H., Andreassen, T., Goksøyr, A., Bruheim, P., Brautaset, T., 2010. Biosynthetic pathway for γ-cyclic sarcinaxanthin in *Micrococcus luteus*: Heterologous expression and evidence for diverse and multiple catalytic functions of C50 carotenoid cyclases. J. Bacteriol. 192, 5688–5699. https://doi.org/10.1128/JB.00724-10.

MarketsandMarketsTM, 2024. Carotenoids Market [WWW Document]. URL https://www.marketsandmarkets.com/Market-Reports/carotenoid-market-158421566.html. (accessed 2.10.25).

Research, G.V., 2024. Carotenoids Market Size, Share & Trends Analysis Report By Product, By Application (Food, Supplements, Feed, Pharmaceuticals, Cosmetics), By Source, By Region, And Segment Forecasts, 2024 - 2030 [WWW Document]. URL https://www.grandviewresearch.com/industry-analysis/carotenoids-market. (accessed 2.10.25).

Richter, T.K.S., Hughes, C.C., Moore, B.S., 2015. Sioxanthin, a novel glycosylated carotenoid, reveals an unusual subclustered biosynthetic pathway. Environ. Microbiol. 17, 2158–2171. https://doi.org/10.1111/1462-2920.12669.

Rohmah, M., Rahmadi, A., Raharjo, S., 2022. Bioaccessibility and antioxidant activity of β-carotene loaded nanostructured lipid carrier (NLC) from binary mixtures of palm stearin and palm olein. Heliyon 8, e08913. https://doi.org/10.1016/j.heliyon.2022.e08913.

Sandmann, G., 2021. Diversity and origin of carotenoid biosynthesis: its history of coevolution towards plant photosynthesis. New Phytol. 232, 479–493. https://doi.org/10.1111/nph.17655.

Sandmann, G., 2019. Antioxidant protection from UV-and light-stress related to carotenoid structures. Antioxidants 8, 219. https://doi.org/10.3390/antiox8070219.

Sasaki, Y., Eng, T., Herbert, R.A., Trinh, J., Chen, Y., Rodriguez, A., Gladden, J., Simmons, B.A., Petzold, C.J., Mukhopadhyay, A., 2019. Engineering *Corynebacterium glutamicum* to produce the biogasoline isopentenol from plant biomass hydrolysates. Biotechnol. Biofuels 12, 41. https://doi.org/10.1186/s13068-019-1381-3.

Schmitt, I., Meyer, F., Krahn, I., Henke, N.A., Peters-Wendisch, P., Wendisch, V.F., 2023. From Aquaculture to Aquaculture: Production of the Fish Feed Additive Astaxanthin by *Corynebacterium glutamicum* Using Aquaculture Sidestream. Mol. 28, 1996. https://doi.org/10.3390/molecules28041996.

Seeger, J., Wendisch, V.F., Henke, N.A., 2023. Extraction and purification of highly active astaxanthin from *Corynebacterium glutamicum* fermentation broth. Mar. Drugs 21, 530. https://doi.org/10.3390/md21100530.

Seeger, J., Zäh, M., Wendisch, V.F., Brandenbusch, C., Henke, N.A., 2025. Supercritical carbon dioxide extraction of astaxanthin from *Corynebacterium glutamicum*. Bioresour. Bioproc. 12, 46. https://doi.org/10.1186/s40643-025-00882-9.

Seel, W., Baust, D., Sons, D., Albers, M., Etzbach, L., Fuss, J., Lipski, A., 2020. Carotenoids are used as regulators for membrane fluidity by *Staphylococcus xylosus*. Sci. Rep. 10, 330. https://doi.org/10.1038/s41598-019-57006-5.

Sen, S., Chakraborty, R., 2011. The Role of Antioxidants in Human Health. In: Andreescu, S., Hepel, M. (Eds.), Oxidative Stress: Diagnostics, Prevention, and Therapy. American Chemical Society, pp. 1–37. https://doi.org/10.1021/bk-2011-1083.ch001.

Sigurdson, G.T., Tang, P., Giusti, M.M., 2017. Natural Colorants: Food Colorants from Natural Sources. Annual Review of Food Science and Technology 8, 261–280. https://doi.org/10.1146/annurev-food-030216-025923.

Tekin, K., Hao, N., Karagoz, S., Ragauskas, A.J., 2018. Ethanol: A Promising Green Solvent for the Deconstruction of Lignocellulose. ChemSusChem 11, 3559–3575. https://doi.org/10.1002/cssc.201801291.

Tsuge, Y., Kawaguchi, H., Yamamoto, S., Nishigami, Y., Sota, M., Ogino, C., Kondo, A., 2018. Metabolic engineering of *Corynebacterium glutamicum* for production of sunscreen shinorine. Biosci. Biotechnol. Biochem. 82, 1252–1259. https://doi.org/10.1080/09168451.2018.1452602.

Xiang, S., Usunow, G., Lange, G., Busch, M., Tong, L., 2007. Crystal structure of 1-deoxy-D-xylulose 5-phosphate synthase, a crucial enzyme for isoprenoids biosynthesis. J. Biol. Chem. 282, 2676–2682. https://doi.org/10.1074/jbc.M610235200.

Zahoor, A., Lindner, S., Wendisch, V.F., 2012. Metabolic engineering of *Corynebacterium glutamicum* aimed at alternative carbon sources and new products. Comput. Struct. Biotechnol. J. 3, e201210004. https://doi.org/10.5936/csbj.201210004.